370 KSME International Journal, Vol. 12, No. 3, pp. 370~379, 1998

Evaluation on the Fracture Toughness and Strength of Fiber Reinforced Brittle Matrix Composites

Yong-Hoon Cha*, Kyoung-Suk Kim* and Duck-Joong Kim**

(*Received June 13, 1997*)

It is well known in the fracture mechanics community that the performance of brittle materials, such as different types of ceramics which have low fracture toughness, improves significantly when fibers are added into the material. This is because the presence of fibers deters the crack propagation. Fibers bridge the gap between two adjacent surfaces of the crack and reduce the crack tip opening displacement, thus make it harder to propagate. Several investigators have experimentally studied how the length, diameter and volume fraction of fibers affect the fracture toughness of fiber reinforced brittle matrix composite materials. However, to this date not much work has been done to develope a micro-mechanics based simplified mathematical model of fiber reinforced composites that can quantitatively explain the increase of the fracture toughness and strength of a composite with volume fraction, length and diameter of fibers, used for strengthening the composite, this is what is attempted in this paper.

Key Words: Stress Intensity Factor, Fracture Toughness, Fiber Reinforced Brittle Matrix Composites, Crack Opening Displacement

1. Introduction

Ward et. al. (1989) studied fracture resistance of acrylic fiber reinforced mortar in shear and flexure and found that as the volume fraction of fibers increases the strength is in shear and flexure, the fracture energy and the critical crack opening increase, the tensile strength remains essentially constant and the compressive strength shows some reduction. Luke, Waterhouse and Wooldridge (1974) investigated the effect of several variables of steel fibers on the flexural strength of concrete. They studied the effect of fiber length, diameter, shape and volume fraction on the first crack strength (the point at which the load-deflection curve deviates from linearity) and ultimate strength of concrete. They concluded from their experimental investigation that the fiber length, fiber diameter, fiber shape and fiber volume fraction affects the flexural strength of the concrete. Longer lengths, smaller diameters, and higher volume fraction of fibers independently improve the ultimate strength of fiber reinforced concrete.

Luke et. al. (1974) have shown in Table 1 that the ultimate flexural strength of fiber reinforced concrete increases from 910 psi to 1880 psi (107% increase) as the fiber volume fraction increases from 0.3% to 2.5% (733% increase). For 1% volume fraction of fibers as the fiber length increases the flexural strength increases from 1190 psi to 1500 psi (26% increase) for 0.01″ diameter fibers, from 1155 psi to 1455 psi (26% increase) for 0.016″ diameter fibers and 1050 psi to 1580 psi (50% increase) for 0.02″ diameter fibers. These three increases correspond to the fiber length increases of 0.5″ to 1.25″ (150% increase), 0.75″ to 2" (167% increase) and 1.5″ to 2.5″ (67% increase) respectively. They have also shown that for 1% volume fraction and 1″ length fibers as the fiber diameter decreases from 0.016″ to 0.006″ (62.5% decrease) the ultimate strength increases from 1115 psi to

* Department of Mechanical Engineering, Chosun University(501-759, Kwangju, Republic of Korea)
** Department of Automotive Engineering, Dong-A College(526-870, Youngam, Chunnam, Republic of Korea)

Table 1 Effect of steel fibers on ultimate strength (σ_U) of reinforced concrete (Luke et. al. 1974).

Fiber parameters that change	change	% change	σ_U change	σ_U change (%)
Volume Fraction (0.3% to 2.5%)	2.2%	733%	970 psi	107%
Length (Diameter=0.01″, v.f.=1%)	0.75″	150%	310 psi	26%
Length (Diameter=0.016″, v.f.=1%)	1.25″	167%	300 psi	26%
Length (Diameter=0.02″, v.f.=1%)	1.0″	67%	530 psi	50%
Diameter (Length=1″, v.f.=1%)	-0.01″	-62.5%	680 psi	61%
Diameter (Length=2″, v.f.=1%)	-0.014″	-46.7%	215 psi	17.3%
Diameter (Length=1″, v.f.=2%)	−0.004″	−25%	175 psi	11.9%

1795 psi (61% increase). For the same volume fraction but for the 2″ length fibers as the fiber diameter decreases from 0.03″ to 0.016″ (46.7% decrease) the ultimate stength increases from 1240 psi to 1455 psi (17.3% increase). On the other hand for 1″ length fibers and 2% volume fraction a decrease of fiber diameter from 0.016″ to 0.012″ (25% decrease) results in an increase in the ultimate strength from 1470 psi to 1645 psi (11.9% increase). They also studied the effect of the shape of fibers and found that flat fibers increase the strength more than round fibers. The increase in the ultimate strength with flat fibers, in comparison with round fibers, was quite significant. This increase varied from 30% to 100% for different lengths and volume fractions of fibers. There was no attempt in the paper to quantitatively predict the change in the ultimate strength or fracture toughness of the composite with the change in the fiber diameter, length, shape or volume fraction. This is what is attempted in this paper. With this goal in mind let us first tabulate the experimental observation of Luke et. al.

2. Theory

The mechanisms responsible for increasing the ultimate strength and fracture toughness when fibers are added, we believe, are essentially same. In brittle materials, like concrete and ceramics, there are a number of micro cracks present in the material. Fibers intersect these micro cracks and bridge the gap between two surfaces of the crack as shown in Fig. 1. Under loading conditions when a crack is willing to propagate, the fibers

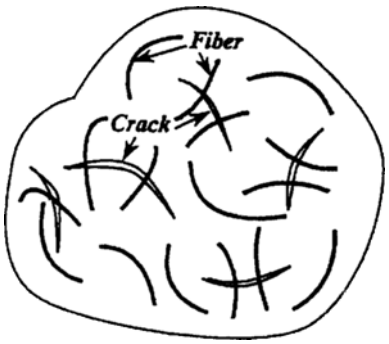

Fig. 1 Fibers bridge the gap between the two surfaces of the cracks.

apply a restraining force, opposing to the crack propagation. Naturally, in presence of fibers the fracture toughness and ultimate strength of the material increases. It is logical to assume that the restraining force applied by the fibers are coming from the friction and cohesive force between the fiber and the matrix material. If this force between the fiber and the matrix be zero then the fibers will not be able to apply any opposing force to the crack propagation. Since the cohesive and friction force increase with the surface area, the flat fibers, which have more surface area than the round fibers for the same volume of fibers, increase the fracture toughness more than the round fibers, which has been experimentally verified [Luke et. al. (1974)].

2.1 Effect of fiber volume fraction

Keeping length and diameter of fibers unchanged if one increases its volume fraction by n% then the restoring force coming from the fibers should increase by n% as well. In Table 1 one can

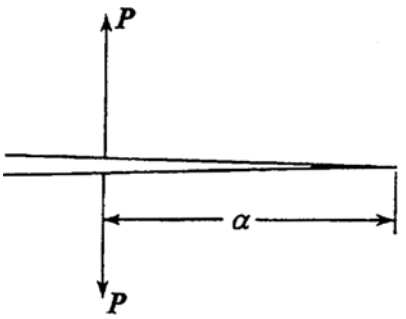

Fig. 2 Semi-infinite crack subjected to loads P at a distance from the crack tip.

see that 733% increase in volume fraction increased the ultimate strength of concrete by only 107%. How can one explain this difference between the volume fraction increase and the ultimate strength increase ? A logical answer to this puzzle can be found from the following consideration. Let us assume that in absence of fibers the matrix material has a fracture toughness of K_c. The fibers bridge the gap between the two surfaces of the crack as shown in Fig. 1 and generate a restoring force when the cracks try to propagate.

The stress intensity factor (SIF) for a semi-infinite crack subjected to two opposing forces as shown in Fig. 2 is given by [Broek (1986)].

$$k_1 = P\sqrt{\frac{2}{\pi\alpha}} \tag{1}$$

Hence, if the SIF due to some loading in absence of the fibers is K then for the same geometry and loading the SIF in presence of fibers which produce the restoring force P would be $(K-k_1)$. Note that K depends on the problem geometry and loading while the k_1 depends on the restoring force magnitude P and the point of application of the restoring force relative to the crack tip. If k_1 is 10% of K then for 100% increase in the fiber volume fraction, the k_1 will be increased by almost a factor of two while K remains unchanged. Thus resulting SIF becomes $(K-2k_1)$. Hence, if the matrix still fails when the resulting SIF reaches the value K_c then the failure criterion in absence and in presence of fibers would be

Fig. 3 Fibers located ahead of the crack tip.

$$\begin{aligned} &K = K_c \text{ (in absence of fibers)} \\ &K - k_1 = K_c \text{ (in presence of some fibers)} \\ &K - 2k_1 = K_c \text{ (for 100\% increase of the fiber volume)} \end{aligned} \tag{2}$$

Clearly if k_1 is 10% of K then the failure load increase will be about only 10% for a 100% increase in the volume fraction of fibers. This increase is only due to the bridging effects of fibers. However, presence of fibers in front of the crack tip as shown in Fig. 3 also increases K_c by some amount, the exact amount of increase depends on the fiber distribution (spacing) ahead of the crack tip [Evans et. al. (1988, 1989, 1991) and Evans and Zok (1994)]. Thus if one accounts for both bridging effect and the effect of fibers ahead of the crack tip then the failure criteria becomes

$$\begin{aligned} &K = K_c \text{ (in absence of fibers)} \\ &K - k_1 = K_c^* \text{ (in presence of some fibers)} \\ &K - 2K_1 = K_c^{**} \text{ (for 100\% increase of the fiber volume)} \end{aligned} \tag{3}$$

where K_c^* and K_c^{**} are critical SIF_s of the composite due to the presence of fibers in front of the crack tip. In this case 100% increase in the fiber volume fraction will increase the ultimate strength by more than 10%. Hence 107% increase in the ultimate strength for 733% increase in the fiber volume fraction is possible.

2.2 Effect of the fiber distribution

If we simply assume that the fiber-matrix interface force is proportional to the interface area between the fiber and the matrix and fracture toughness is increased due to this force alone, then keeping the volume fraction and fiber diameter unchanged but increasing the fiber length will not affect the interface area and the fracture toughness, however it does have a big influence on the ultimate strength as shown in Table 1.

Table 1 shows that 26% and 50% increase in the ultimate strength is achieved by increasing the fiber length by 167% and 50% respectively. Hence, in addition to the matrix-fiber interface cohesive force, some other mechanism must play an important role in deciding the strength of the composite.

In addition to the fiber surface area, distribution of fibers relative to the crack may also play an important role in deciding the level of resistance to the crack propagation. To investigate the effect of the fiber distribution on the SIF of a cracked material, the SIF of a semi-infinite crack in an infinite medium is computed with and without the fiber forces. As mentioned before the SIF for the geometry shown in Figs. 2 and 4(a) is given by

$$k_1 = P\sqrt{\frac{2}{\pi a}}$$

SIF for the problem geometry shown in Fig. 4 (b) can be obtained from Eq. (1) by superposition

$$k_1 = \frac{P}{2}\sqrt{\frac{2}{\pi(a-\varepsilon)}} + \frac{P}{2}\sqrt{\frac{2}{\pi(a+\varepsilon)}} = P\frac{\sqrt{a+\varepsilon}+\sqrt{a-\varepsilon}}{\sqrt{2\pi(a^2-\varepsilon^2)}} \tag{4}$$

For $\varepsilon = a/2$, k_1 of Eq. (4) becomes 1.116P $(2/\pi a)^{0.5}$. This is an increase of 11.6% of the stress intensity factor compared to Eq. (1). Hence, if a cracked infinite plate has a SIF of K in absence of any fiber, then addition of fibers will reduce the SIF to $(K-k_1)$ if one fiber applies a closing force P(in this case the fiber force will be opposite to that shown in Fig. 4(a)). The SIF will then be reduced to (K-1. $116k_1$) if two fibers, instead of one fiber, apply a total load of P as shown in Fig. 4(b). Distributing the total force P over a larger number of fibers does not always reduce the SIF. For example, when the load is distributed over four fibers, each carrying P/4 as shown in Fig. 4(c), the SIF becomes 1.101P$(2/\pi a)^{0.5}$ an increase of 10.1% as opposed to 11.6% for the two fiber case. If the load is distributed over eight fibers as shown in Fig. 2(d) the SIF becomes 1.15P$(2/\pi a)^{0.5}$, a 15% difference from Eq. (1). If one accepts this model of fiber force generation then, from the above analysis, one should conclude that 10 to 15% difference in the fracture toughness may be attributed to the effect of fiber distribution unless the distribution is such that some fibers go through the crack tip, thus making $a=0$ and $k=\infty$.

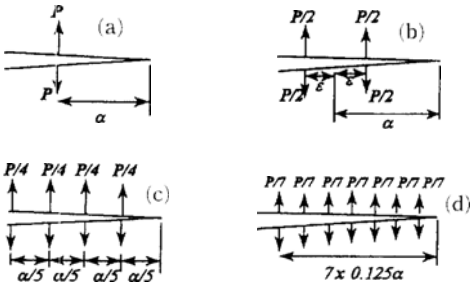

Fig. 4 Semi-infinite cracks subjected to a resultant opening load P at a distance a from the crack tip when the load act at (a) one point, (b) two points, (c) four points and (d) seven points.

To see if this conclusion is also valid for finite cracks the SIFs for the problem geometries shown in Fig. 5 are computed as well For the geometry shown in Fig. 5(a) the SIF is given by [Tada et. al. (1973)].

$$k_1 = \frac{2P}{[\pi a(1-(b/a)^2]}F(b/a) \tag{5}$$

Where $F(b/a)$ changes from 1.3 to 1.0 as b/a varies between 0 to 1.

For two forces of magnitudes P/2 acting as shown in Fig. 5(b), the SIF is given by

$$k_1 = nP/\sqrt{\pi a} \tag{6}$$

where n is given in Table 2.

Note that $b_1 : b_2 = 5 : 5$ simply means one force P acting at the mid point as shown in Fig. 5(a). Applying the force to four equally spaced forces of magnitude P/4 or seven equally spaced forces of magnitude P/7 change the factor n to 2.94 and 3.03 respectively. Hence, this exercise also shows a maximum increase of 11.5% in SIF with varying distribution of fibers.

Table 2 n of Eq. (6) for different values of $b_1 : b_2$ of Fig. 5(b).

$b_1 : b_2$	5 : 5	4 : 6	3 : 7	2 : 8	2.5 : 7.5
n	2.77	2.79	2.9	3.09	2.97

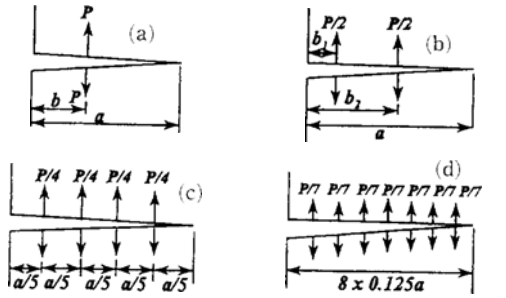

Fig. 5 A finite crack of length "a" in an infinite medium is subjected to a resultant opening load P when the loads act at (a) one point, (b) two points, (c) four points and (d) seven points.

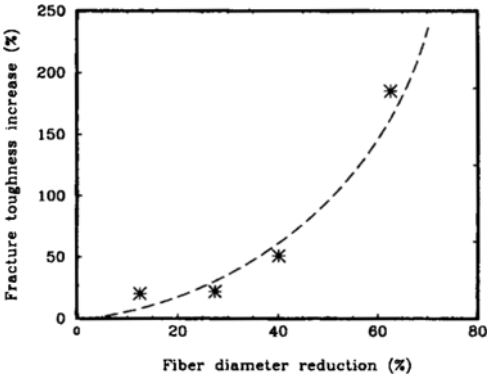

Fig. 6 Theoretical prediction of the percentage increase (X) of the fracture toughness as a function of the percentage reduction (n) of the fiber diameter.

2.3 Effect of fiber diameter

While keeping the volume fraction and fiber length unchanged if one reduces the fiber diameter then the number of fibers increase, causing an increase in the fracture toughness and ultimate strength. It is easy to see that n% reduction in the fiber diameter causes n% reduction in the fiber surface area. If the coefficient of friction between the fiber surface and the matrix does not change then the force produced by individual fibers will be reduced by n%. Then the individual fiber's cross sectional area and volume are reduced by m%, where

$$m = 100\left[1 - \left(1 - \frac{n}{100}\right)^2\right] \tag{7}$$

For the same volume fraction and length the number of fibers is then increased by [m/(100 -m)]% for the n% reduction of the fiber diameter. Hence, if the increase in the restoring force is X% due to n% reduction of diameter then

$$X = m\left(\frac{100 - n}{100 - m}\right) - n \tag{8}$$

A plot of n versus X is shown in Fig. 6. Since restoring force is directly propotional to the SIF K, Fig. 6 shows the variation of k_1 (the part of SIF that depends on the fibers, see Eq. (2)) with n. However, the total SIF has two parts K and k_1 as shown in Eq. (2) and (3). An increase in k_1 reduces the total SIF $(K\text{-}k_1)$, since K depends only on the loading and the problem geometry and not on fiber geometry. As k_1 increases, since SIF decreases, the critical load for failure and the ultimate strength should increase. From Fig. 6 one can see that as n increases from 0 to 70%, X increases from 0 to 240%, monotonically with increasing slop. Experimental results show that as n is increased by 25%, 46.7% and 62.5%, the ultimate strength is increased by 11.9%, 17.3% and 61% respectively, with a monotonic increase for different volume fraction and fiber lengths. Since X of Fig. 6 shows the variation of k_1 and values listed in Table 1 correspond to the variation of σ_u we do not expect them to be numerically equal. However, they should follow the same trend and that is what they do. If we consider constant fiber length (1 inch) and volume fraction (1%) and reduce the fiber diameter by 12.5%, 25%, 37.5% and 62.5% then the ultimate strength increases by 9%, 10.3%, 18.4% and 61% (Luke et. al. 1974). If one plots these experimental values with a different scale (shown on the right side of the figure) on the same figure then one can see that they match very well with the theoretical curve. Clearly the experimental results support our theory.

2.4 Effect of fiber length

As mentioned before, cohesive force and friction force between fibers and matrix is an important factor for increasing the fracture toughness of the fiber reinforced materials but is not the only factor. If it were the only factor then changing fiber length but keeping the volume fraction and

fiber diameter constant would not have any effect on the ultimate strength, because the overall restoring force is not altered when the fiber length is decreased by n% and the number of fibers is increased by the same amount. When the number of fibers is increased the restoring fiber forces are redistributed as shown in Fig. 4. Hence, with decreasing fiber lengths the fracture toughness should increase slightly because as we have seen earlier distributing the loads over a region instead of a point increases K by 10 to 15% unless some of these forces are applied very close to the crack tip, making α close to zero. However, experimentally we observe that the opposite is true, i. e. the fracture toughness increases with the increase in the fiber length when the fiber diameter and volume fraction are kept constant.

Our explanation to this apparently contradictory results is the following. For short fibers the fibers remain more or less straight, as shown in Fig. 7, and the fiber forces may be assumed to be proportional to the fiber length. However the long fibers do not remain straight. They may wrap around the aggregates or bend themselves differently as shown in Fig. 7. Hence the fiber force is not necessarily proportional to the fiber length. For a short fiber it may be simply proportional to the interface area between the fiber and the matrix, but for long fibers if the fibers are properly wrapped around the aggregates such that they cannot slip then the fiber force should be proportional to its stiffness and tensile strength instead of its surface area. If the theory proposed here to explain the increase of the fracture toughness of the composite with the increase of fiber length is true then the fracture toughness should initially increase with the fiber length, however, after this length reaches some critical value necessary for properly wrapping it around the aggregate, further increase of fiber length would not increase the fracture toughness.

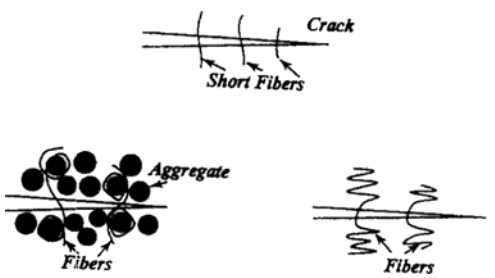

Fig. 7 Possible orientations of short fibers and relatively long fibers that bridge the gab between two crack surfaces.

Majumdar and Nurse(1978) observed that for glass fiber reinforced cement composites the modulus of rupture and impact strength increase markedly up to 30 mm glass fiber length, but those change very little when the fiber length is increased from 30 to 40 mm. Hence, their results support our theory. Obviously the critical fiber length depends on the aggregate size and should change from one mix to another if the aggregate size changes.

2.5 Effect on stiffness

The mechanism of fiber resisting the crack propagation has the direct effect on the increase of the fracture toughness, which indirectly increases the ultimate strength. However, increase in the fracture toughness should not have much influence on the stiffness of the material. Hence, the Young's modulus should remain unchanged, or should vary a little when short fibers are added to strengthen the composite.

3. Experimental Methods

3.1 Composite materials

The composite matrix is made of lunar simulants or artificial moon rocks. Two types of lunar simulants have been adopted within last few years to simulate regolith. These are Arizona Lunar Simulant, ALS [Desai and Girdner, 1992] and Minnesota Lunar Simulant, MLS [Weiblein and Gordon, 1988]. Both ALS and MLS have properties similar to those of regolith. The rock was crushed and then sieved. The sieved fractions were mixed to match the grain size distribution of actual lunar soil brought by APOLLO missions.

Figure 8 shows grain size distribution of ALS, chemical composition is given in Table 3.

3.2 Specimen preparation

The ALS powder is poured in a specially

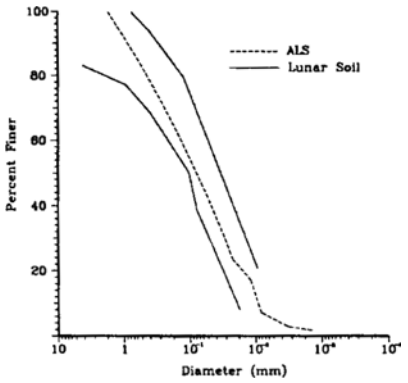

Fig. 8 Grain size distribution of ALS.

Table 3 Chemical composition for simulants and lunar soils (wt. %).

Compound	Simulants		Lunar soils	
	ALS	MLS	MARE	HIGHLANDS
SiO_2	48.0–50.0	43.86	45.4	45.5
AL_2O_3	13.5–16.0	13.68	14.9	24.0
TiO_2	1.6–3.2	6.32	3.9	0.6
FeO	7.0–12.5	13.4	14.1	5.9
MnO	0.2–0.25	0.198	—	—
Mgo	4.3–6.5	6.68	9.2	7.5
CaO	8.3–10.3	10.13	11.8	15.9
Na_2O	2.7–3.0	2.12	0.6	0.6
K_2O	0.5–1.5	0.281	—	—
Fe_2O_3	1.9–4.6	2.6	—	—
P_2O_5	—	0.2	—	—
CO_2	—	0.0015	—	—

designed mold and heated at a rate of 3°C per minute to 1100°C in a 1700°C capacity furnace, see Fig. 9 [Toth and Desai (1994)]. At 150°C there is a two hour waiting period so that the sample becomes fully dry before it is heated further. The entire heating and cooling process takes an average of seven hours, as shown in Fig. 10. The ALS brick thus prepared is cut into 6.2″×1.26″×0.67″ size specimens and a crack of length 0.63″ is cut at the center, see Fig. 11. There types of specimens are prepared-ALS with Carbon Steel (CS) fibers (fiber dimension : 1″×0.09″×0.02″), ALS with Stainless Steel(SS) fibers (fiber dimension : 0.6″×0.03″×0.01″) and ALS without

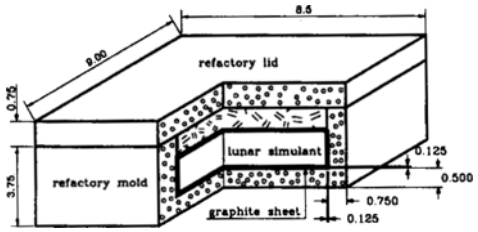

Fig. 9 Mold for flat specimen.

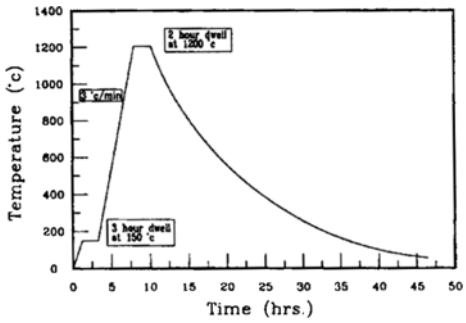

Fig. 10 Temperature history during heating and cooling.

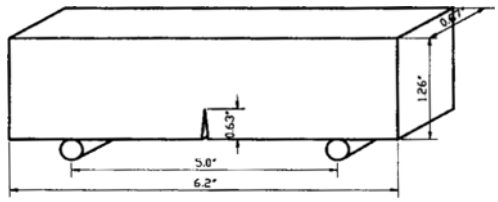

Fig. 11 Specimen geometry for the 3-point bending test.

fibers. The fiber weight is 10% of the ALS weight.

Although attempts have been made to uniformly distribute the fibers in the ALS matrix some variations always exist from one specimen to the next since ALS powder and fibers are mixed, very crudely, by hands. Two specimens(A and B) of each type of composites are prepared and tested to get an idea about the scatter about the mechanical properties of these crudely prepared specimens. Three point bend specimens are prepared by cutting the composite blocks to the desired shape, see Fig. 11. The specimen is loaded at the mid point above the crack with two simple supports at the two ends, five inch apart.

4. Results and Discussion

Effect of different parameters of fibers on the ultimate strength of a brittle matrix composite has been discussed above and compared with the experimental results. In this section some additional expeimental results are presented with a new type of ceramic matrix composite specimens. These experimental results show that the fiber addition increases the fracture toughness strongly but it has very weak effect on the stiffness of the composite

4.1 Load-displacement diagrams

Load-displacement diagrams of ALS without fibers, ALS-CS and ALS-SS composites are shown in Figs. 12, 13 and 14 respectively. Figures 13 and 14 include two plots in each figure. Two plots show response of two specimens (A and B) having the same amount of fibers. Ideally these two plots should be indentical. However, in reality they show significant differences, especially after the peak stress is reached. These differences are due to nonuniform distribution of fibers and voids in the specimens. In spite of these differences, one can clearly see that there is a significant increase of the peak loads of ALS-SS composites compared to ALS or ALS-CS composites. CS fibers only slightly increased the peak load from 75 lb (for pure ALS) to 78 lb and 88 lb for two ALS-CS specimens. However, SS fibers increased the peak load to 138 lb and 188 lb for the two specimens.

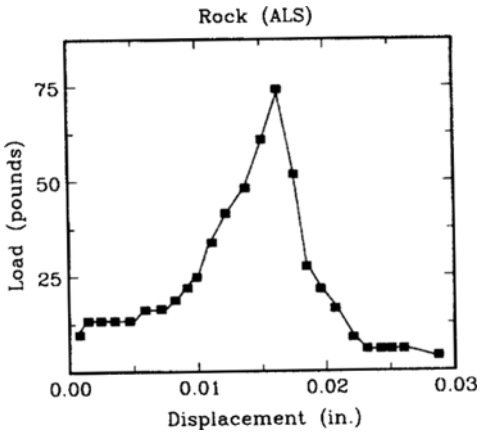

Fig. 12 Load-displacement diagram obtained form the 3-point bending of ALS specimen.

4.2 Critical stress intensity factor

Fracture toughness or critical SIFs (K_c) calculated from the peak loads for the specimen geometry shown in Fig. 15 are tabulated in Table 4 along with the peak load values.

Clearly almost 150% increase in the fracture toughness is possible by simply adding 10% weight fraction of stainless steel fibers. However, the Young's modulus of the specimens do not show such large variations; ALS, ALS-CS and ALS-SS specimens have Young's modulus

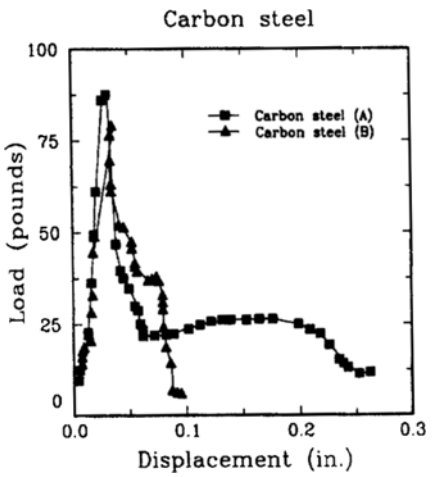

Fig. 13 Load-displacement diagram obtained form the 3-point bending of ALS-CS specimen.

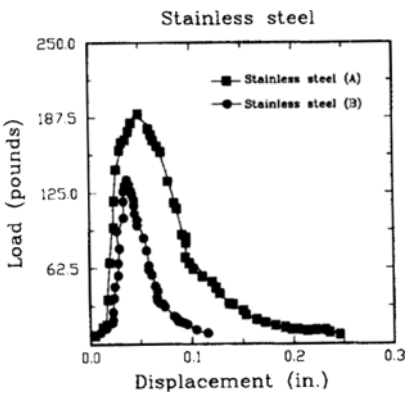

Fig. 14 Load-displacement diagram obtained form the 3-point bending of ALS-SS specimen.

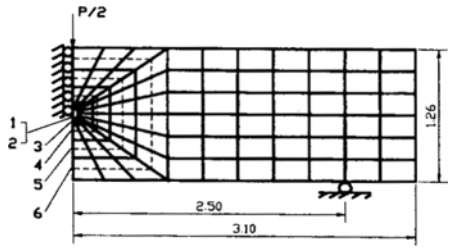

Fig. 15 Finite-element mesh and six J-integral paths.

Table 4 Peak loads and K_c for five specimens made of lunar simulant matrix.

Specimen	ALS	ALS-CS (A)	ALS-CS (B)	ALS-SS (A)	ALS-SS (B)
Peak load (lb)	75	88	78	188	138
K_c (lb-in$^{3/2}$)	1029.6	1208.0	1070.8	2580.9	1894. 4

approximately equal to 3500, 3500 and 4000 ksi respectively. Hence, less than 15% increase in stiffness is achieved in this manner.

What is interesting to note here is that SS -fibers have the cross sectional area one-sixth of that of CS fibers and their length is 60% of the CS -fibers. These differences in dimensions may cause some difference in the fracture toughness as discussed earlier. However, the main reason for this difference is not the change in fiber dimensions but the fiber-matrix interface condition. At the high liquefaction temperature rusts are formed at the CS fiber boundaries making th fiber-matrix bonds weak. SS fibers on the other hand do not form any rust thus the fiber-matrix bond is much stronger in this case. That is why CS fibers in specimen B improved the fracture toughness by less than 5%. Besides rusting, another factor that negatively affected the ALS-CS composite is nonuniform fiber distribution. Since CS-fibers are bigger and heavier compared to SS-fibers, heavy concentration of CS-fibers was observed near the lower half of the specimen. Hence, at the upper half, ahead of the crack tip, CS-fibers had much lower weight fraction. SS-fibers being smaller and lighter were distributed more uniformly.

The central crack starts to propagte when the peak load is reached. Hence, one can calculate the

Table 5 J_c and K_c for the five specimens.

Specimen type		ALS	ALS-CS		ALS-SS	
			A	B	A	B
Peak load P(lb)		75	88	78	186	138
J_c(lb/in) computed by ABAQUS	Path 1	.1317	.1813	.1424	.2999	.1651
	Path 2	.1288	.1773	.1393	.2934	.1615
	Path 3	.1292	.1779	.1398	.2944	.1620
	Path 4	.1296	.1780	.1399	.2946	.1621
	Path 5	.1298	.1783	.1401	.2950	.1623
	Path 6	.1303	.1794	.1410	.2969	.1634
Average J_c(lb/in)		.1299	.1787	.1404	.2957	.1627
K(lb/in-3/2)		702.37	823.81	730.21	1160.86	861.09

critical J-integral value J_c from the specimen geometry and the peak load. ABAQUS finite element program is used to calculate J_c. The finite element mesh that was used in this analysis is shown in Fig. 15. J_c was calculated along six paths 1-6 shown in Fig. 15. Since J_c and K_c (critical stress intensity factor) are related ($J_c = \alpha K_c^2/E$, $\alpha = 1$ for plane stress and $\alpha = (1-\nu)^2$ for plane strain, ν = Poission's ratio) one can obtain K_c from J_c. These values are shown in Table 5.

5. Conclusions

In this paper theoretical and experimental investigations are carried out to study the effects of fibers on the fracture toughness, ultimate strength and stiffness of brittle matrix composites. It is observed that the fibers, if bonded properly with matrix, increase the strength and fracture toughness of a composite significantly but do not have much effect on its stiffness. Fracture toughness increases almost propotionately with the fiber volume fraction and it increases nonlinearly with the fiber length. Theory predicts that after some critical length further increase of the fiber length should not increase the fracture toughness and ultimate strength of the composite, that is what is ovserved experimentally as well. Fracture toughness and ultimate strength also increase nonlinearly with the decrease of the fiber diameter when other parameters are unaltered. Theoreti-

cal results show that the rate or slope of the fracture toughness variation monotonically increas with the reduction of the fiber diameter. Experimental results support this theoretical prediction.

Good fiber-matrix bonding is necessary for the increase of the fracture toughness of the composite with the fiber addition. If the bonding strength is not high enough, the increase of the fracture toughness due to addition of fibers is insignificant.

References

Broek, D., 1986, *Elementary Engineering Fracture Mechanics,* 4th Edition, Pub. Martinus Nijhoff.

Desai, C. S., and Girdner, K. 1992, "Structural Materials From Lunar Simulants Through Thermal Liquefaction," *Proceedings of ASCE Space'92 Conference,* pp. 528~536, Denver, Colorado.

Weilein, P., and Gordon, K. 1988, "Characteristics of a Simulant for Lunar Surface Materials," Lunar Bases and Space Activities in the 21st Century, NASA.

Evans, A. G., 1988, "Mechanical Performance of Fiber Reinforced Ceramic Matrix Composites," *Proceedings of the 9-th Riso International Symposium on Metallurgy and Materials Science,* Pub. Riso Natl. Lab., Riso Library, Roskilde, Den., pp. 13~34.

Evans, A. G., 1989, "High Toughness Ceramics and Ceramic Composites," *Proceedings of the tenth Riso International Symposium on Metallurgy and Materials Science,* Pub. Riso. Natl. Lab., Riso Library, Roskilde, Den., pp. 51~91.

Evans, A. G., 1991, "Mechanical Properties of Reinforced Ceramic, Metal and Intermetallic Matrix Composites," *Materials Science and Engineering A:* Structural Materials: Properties, Microstructure and Processing, Vol. A143, pp. 63~76.

Evans, A. G., Zok, F. W., 1994, "Physics and Mechanics of Fiber-Reinforced Brittle Matrix Composites," *Journal of Materials Science,* Vol. 29, pp. 3857~3896.

Luke, C. E., Waterhouse, B. L., and Wooldridge, J. F., 1974, "Steel Fiber Reinforced Concrete Optimization and Applications," *An Inteneational Symposium on Fiber Reinforced Concrete,* Pub. American Concrete Institute, Detroit, Michigan, SP-44, pp. 393~413.

Majumdar, A. J., and Nurse, R. W., 1978, "Glass Fiber Reinforced Cement," *BRE Building Research Series,* Vol. 2, pp. 77~94, Pub. The Construction Press Ltd., Lancaster, England.

Tada, H, Paris P. C., and Irwin, G. R., 1973, *The Stress Analysis of Cracks Handbook,* Pub. Del Research Corporation, Hellertown, PA, USA.

Toth, J. C., and Desai, C. S., "Development, Testing and Modeling of Ceramic Composites for Lunar Applications," *Proceedings of ASCE Space '94 Conference,* Albuquerque, New Mexico.

Ward, R. J., Yamanobe, K, Li, V. C., and Backer, S., 1989, "Fracture Resistance of Acrylic Fiber Reinforce Mortar in Shear and Flexure," in *Fracture Mechanics: Application to Concrete,* Eds. V. C. Li and Z. P. Bazant, Pub. ACI, Vol. SP 118-2, pp. 17~68.